

Argonne National Laboratory

**EXPERIMENTAL INVESTIGATIONS OF
SECONDARY CRITICAL CONFIGURATIONS
(ZPR-III Assemblies 27 and 28)**

by

**W. Gemmell, J. K. Long,
and W. P. Keeney**

LEGAL NOTICE

This report was prepared as an account of Government sponsored work. Neither the United States, nor the Commission, nor any person acting on behalf of the Commission:

A. Makes any warranty or representation, expressed or implied, with respect to the accuracy, completeness, or usefulness of the information contained in this report, or that the use of any information, apparatus, method, or process disclosed in this report may not infringe privately owned rights; or

B. Assumes any liabilities with respect to the use of, or for damages resulting from the use of any information, apparatus, method, or process disclosed in this report.

As used in the above, "person acting on behalf of the Commission" includes any employee or contractor of the Commission, or employee of such contractor, to the extent that such employee or contractor of the Commission, or employee of such contractor prepares, disseminates, or provides access to, any information pursuant to his employment or contract with the Commission, or his employment with such contractor.

ANL-6866
Reactor Technology
(TID-4500, 37th Ed.)
AEC Research and
Development Report

ARGONNE NATIONAL LABORATORY
9700 South Cass Avenue
Argonne, Illinois 60440

EXPERIMENTAL INVESTIGATIONS OF
SECONDARY CRITICAL CONFIGURATIONS
(ZPR-III Assemblies 27 and 28)

by

W. Gemmell,*J. K. Long, and W. P. Keeney

Idaho Division

*Assigned to Argonne National Laboratory from the United Kingdom Atomic Energy Authority. Present Address: Australian Atomic Energy Commission, Lucas Heights, N.S.W.

November 1964

Operated by The University of Chicago
under
Contract W-31-109-eng-38
with the
U. S. Atomic Energy Commission

TABLE OF CONTENTS

	<u>Page</u>
ABSTRACT	9
I. INTRODUCTION.	9
II. DESCRIPTION OF ZPR-III.	12
III. ASSEMBLY 27	13
A. Approach to Critical.	15
B. Fission Rate Traverses.	16
C. Reactivity Worth Traverses	20
IV. ASSEMBLY 28	28
A. Approach to Critical.	30
B. Fission Rate Traverses.	31
C. Reactivity Worth Traverses	33
REFERENCES	38
ACKNOWLEDGMENT	38

LIST OF FIGURES

<u>No.</u>	<u>Title</u>	<u>Page</u>
1.	Interface Views of Assemblies 27 and 28	11
2.	General View of ZPR-III in Shutdown Condition	12
3.	Assembly 27, Typical Drawer with Dense and Normal Core, and Blanket.	13
4.	Assembly 27, Typical Drawer with Void, Normal Core, and Blanket.	13
5.	Assembly 27, Top and Interface View of Assembly.	14
6.	Assembly 27, Representative View through Cross Section of Core.	14
7.	Assembly 28/27, Front Views of Core and Blanket Regions of Traverse Drawer	16
8.	Assembly 27, Axial U ²³⁵ Fission Counter Traverse.	19
9.	Assembly 27, Radial U ²³⁵ Fission Counter Traverse; Axial Position, 1.09 in.	19
10.	Assembly 27, Radial U ²³⁵ Fission Counter Traverse; Axial Position, 3.26 in.	19
11.	Assembly 27, Radial U ²³⁵ Fission Counter Traverse; Axial Position, 5.44 in.	19
12.	Assembly 27, Radial U ²³⁵ Fission Counter Traverse; Axial Position, 7.61 in.	19
13.	Assembly 27, Radial U ²³⁵ Fission Counter Traverse; Axial Position, 9.79 in.	20
14.	Assembly 27, Radial U ²³⁵ Fission Counter Traverse; Axial Position, 14.14 in.	20
15.	Assembly 27, Radial U ²³⁵ Fission Counter Traverse; Axial Position, 20.67 in.	20
16.	Assembly 27, Axial Worth Traverse; Sample: 0.5-in. U ²³⁵ . . .	23
17.	Assembly 27, Axial Worth Traverse; Sample: 1-in. Natural Uranium	24
18.	Assembly 27, Axial Worth Traverse; Sample: 2-in. U-mixed.	24
19.	Assembly 27, Radial Worth Traverse; Sample: 0.5-in. U ²³⁵ ; Axial Position, 1.09 in.	25

LIST OF FIGURES

<u>No.</u>	<u>Title</u>	<u>Page</u>
20.	Assembly 27, Radial Worth Traverse; Sample: 0.5-in. U ²³⁵ ; Axial Position, 3.26 in.	25
21.	Assembly 27, Radial Worth Traverse; Sample: 0.5-in. U ²³⁵ ; Axial Position, 5.44 in.	25
22.	Assembly 27, Radial Worth Traverse; Sample: 0.5-in. U ²³⁵ ; Axial Position, 7.16 in.	25
23.	Assembly 27, Radial Worth Traverse; Sample: 0.5-in. U ²³⁵ ; Axial Position, 9.79 in.	25
24.	Assembly 27, Radial Worth Traverse; Sample: 0.5-in. U ²³⁵ ; Axial Position, 14.14 in.	25
25.	Assembly 27, Radial Worth Traverse; Sample: 0.5-in. U ²³⁵ ; Axial Position, 20.67 in.	26
26.	Assembly 27, Radial Worth Traverse; Sample: 2-in. U-mixed; Axial Position, 1.09 in.	26
27.	Assembly 27, Radial Worth Traverse; Sample: 2-in. U-mixed; Axial Position, 3.26 in.	26
28.	Assembly 27, Radial Worth Traverse; Sample: 2-in. U-mixed; Axial Position, 5.44 in.	26
29.	Assembly 27, Radial Worth Traverse; Sample: 2-in. U-mixed; Axial Position, 7.61 in.	26
30.	Assembly 27, Radial Worth Traverse; Sample: 2-in. U-mixed; Axial Position, 9.79 in.	26
31.	Assembly 27, Radial Worth Traverse; Sample: 2-in. U-mixed; Axial Position, 14.14 in.	27
32.	Assembly 27, Radial Worth Traverse; Sample: 2-in. U-mixed; Axial Position, 20.67 in.	27
33.	Assembly 28, Typical Core Drawer	28
34.	Assembly 28, Top and Interface View of Assembly	28
35.	Assembly 28, Representative View through Core Cross Section	29
36.	Assembly 28, Core Configurations Used in Estimating Critical Mass	30
37.	Assembly 28, Axial U ²³⁵ Fission Counter Traverse.	35
38.	Assembly 28, Radial U ²³⁵ Fission Counter Traverse; Axial Position, 1.09 in.	35

LIST OF FIGURES

<u>No.</u>	<u>Title</u>	<u>Page</u>
39.	Assembly 28, Radial U ²³⁵ Fission Counter Traverse; Axial Position, 3.26 in.	35
40.	Assembly 28, Radial U ²³⁵ Fission Counter Traverse; Axial Position, 5.44 in.	35
41.	Assembly 28, Radial U ²³⁵ Fission Counter Traverse; Axial Position, 7.61 in.	35
42.	Assembly 28, Radial U ²³⁵ Fission Counter Traverse; Axial Position, 9.79 in.	35
43.	Assembly 28, Axial Worth Traverse; Sample: 0.5-in. U ²³⁵ . . .	36
44.	Assembly 28, Axial Worth Traverse; Sample: 2-in. U-mixed.	36
45.	Assembly 28, Radial Worth Traverse; Sample: 0.5-in. U ²³⁵ ; Axial Position, 1.09 in.	36
46.	Assembly 28, Radial Worth Traverse; Sample: 0.5-in. U ²³⁵ ; Axial Position, 3.26 in.	36
47.	Assembly 28, Radial Worth Traverse; Sample: 0.5-in. U ²³⁵ ; Axial Position, 5.44 in.	36
48.	Assembly 28, Radial Worth Traverse; Sample: 0.5-in. U ²³⁵ ; Axial Position, 7.61 in.	36
49.	Assembly 28, Radial Worth Traverse; Sample: 0.5-in. U ²³⁵ ; Axial Position, 9.79 in.	37
50.	Assembly 28, Radial Worth Traverse; Sample: 2-in. U-mixed; Axial Position, 1.09 in.	37
51.	Assembly 28, Radial Worth Traverse; Sample: 2-in. U-mixed; Axial Position, 3.26 in.	37
52.	Assembly 28, Radial Worth Traverse; Sample: 2-in. U-mixed; Axial Position, 5.44 in.	37
53.	Assembly 28, Radial Worth Traverse; Sample: 2-in. U-mixed; Axial Position, 7.61 in.	37
54.	Assembly 28, Radial Worth Traverse; Sample: 2-in. U-mixed; Axial Position, 9.79 in.	37

LIST OF TABLES

	<u>Page</u>
I. Approach to Critical, Assembly 27	15
II. Composition, Critical Dimensions and Masses of Assembly 27 by Zones.	16
III. Assembly 27, Axial Traverse, U ²³⁵ Fission Counter, at R = 0.3 in.	17
IV. Assembly 27, Radial Traverses, U ²³⁵ Fission Counter.	18
V. Reactivity Worth Traverse Samples.	20
VI. Assembly 27, Axial Worth Traverses.	22
VII. Assembly 27, Radial Worth Traverses, 0.5-in. U ²³⁵ Sample . .	22
VIII. Assembly 27, Radial Worth Traverses, 2-in. Natural Uranium Sample.	22
IX. Assembly 27, Radial Worth Traverses, 2-in. U-mixed Sample.	23
X. Approach to Critical - Assembly 28.	30
XI. Composition, Critical Dimensions and Masses of Assembly 28 by Zones.	31
XII. Assembly 28, Axial Traverse, U ²³⁵ Fission Counter, at R = 0.3 in.	32
XIII. Assembly 28, Radial Traverses, U ²³⁵ Fission Counter.	32
XIV. Assembly 28, Axial Sample Worth Traverses	33
XV. Assembly 28, Radial Worth Traverses, 0.5-in. U ²³⁵ Sample . .	34
XVI. Assembly 28, Radial Worth Traverses, 2-in. U-mixed Sample.	34

EXPERIMENTAL INVESTIGATIONS OF
SECONDARY CRITICAL CONFIGURATIONS
(ZPR-III Assemblies 27 and 28)

by

W. Gemmell, J. K. Long,
and W. P. Keeney

ABSTRACT

Two configurations of a fast reactor core following a postulated accidental meltdown were investigated. The configurations were chosen to represent nonuniform distributions of fuel in which calculations of flux and reactivity worth could be compared with experimental values. The first configuration, Assembly 27, represented a case in which the center of a core had melted, and the top and center portions had collapsed into a dense fuel mass in the bottom of the reactor. The dense region is then surrounded by an annulus with the normal core composition, and this in turn is surrounded by the normal blanket. The second configuration, Assembly 28, represented a core in which vaporizing sodium caused the expulsion of all material from the axis of the core, and the annulus had melted and collapsed into a dense ring of fuel.

If these situations were encountered in an actual meltdown, a secondary critical or supercritical configuration of fuel could occur. The history of this secondary configuration would be governed by the spatial relationships of the fuel worth, power distribution, and degree of criticality. The relationship of the power and fuel-worth distributions would determine if further motion of the fuel would result in an autocatalytic configuration. The experiments in the Zero Power Reactor III, (ZPR-III) provided fission-rate and reactivity-worth distributions which may be used to evaluate calculational methods designed to describe the history of possible accident configurations.

I. INTRODUCTION

Critical studies for the Enrico Fermi Fast Reactor have been performed at Argonne National Laboratory's ZPR-III facility under a contractual

arrangement [AT(11-1)-476] between the Power Reactor Development Corporation (PRDC) and the United States Atomic Energy Commission. The original series of critical experiments in this program⁽¹⁾ were begun in 1958.

The discussions leading to the PRDC critical program had shown the desirability of meltdown experiments. Meltdown of a fast reactor containing more than 400 kg of enriched U^{235} certainly presents the possibility of formation of a secondary critical configuration. Moreover, in this concentrated reactor, decay heat builds up to a level sufficient to melt the core by its own gamma field in the event of loss of sodium coolant. Although the loss of sodium is almost inconceivable, a realistic examination of the consequences of this type of accident is in order. It was not until 1960 that an experimental program for such an examination was devised to utilize the unique flexibility of the ZPR-III machine and that could contribute in a very general fashion to the safety analysis of fast reactors.

The mathematical treatment of meltdown events is subject to two general areas of complication which lead to uncertainties in the results obtained. The first is the thermal-mechanical problem leading to some sort of collapse of the core. If the time behavior of the core elements during collapse were known, it would be possible to estimate the rate of reactivity increase and, starting from a normal subcritical configuration, to predict at what speed and in what geometry a secondary critical mass would be assembled. The heterogeneous nature of the reactor and the varying physical properties of the supporting structure during collapse are complications which have been a deterrent to an exact treatment of this phase of the problem.

The second area of consideration may be thought of as taking place after a secondary critical configuration has been achieved. If, at this time a fairly large excess of reactivity has been accumulated, the subsequent course of the excursion will be rapid enough that further gravity collapse of the core can be either neglected or very simply approximated as by a linear ramp function. The problem then involves the nuclear reaction calculation with generation of heat, pressure waves, and expansion until the reactor is disassembled. Methods for handling this part of the calculation have been proposed by Bethe and Tait,⁽²⁾ as well as by Jankus⁽³⁾ and Nicholson.⁽⁴⁾

It was largely as a result of suggestions by Bethe and Nicholson that it became apparent that ZPR-III critical experiments could best be applied to idealized configurations postulated for the first phase to gain a general understanding of the second phase of the problem. A key point in the problem requires criticality calculations of the nonuniform fuel distribution of the secondary critical mass. Although such calculations are straightforward with high-speed numerical methods, there is probably no previous experimental information available by which to gauge the reliability of the calculations; at least this is true in the case of dilute fast power reactors. The

ZPR-III facility could be used to construct nonuniform fuel distributions which are thought to be typical of possible meltdown configurations, and the criticality calculations verified. Moreover, in the ZPR-III, the patterns of flux and reactivity worth throughout the nonuniform core can be determined experimentally, these patterns being required in subsequent stages of the excursion calculation. In fact, the expansion of the secondary critical mass is governed by the pressure gradient pattern which is closely related to the pattern of the flux gradient. Then, as the reactor expands, the change in k will be governed by the pattern of the gradient of reactivity worth. In general, if the fuel expands into a region of higher worth, the reaction is autocatalytic and considerably more violent than if this does not happen.

Two nonuniform fuel distributions were chosen for study on ZPR-III. Although they are not derived from rigorous calculations of phase one of the problem, they are related in a qualitative way to various courses that a meltdown might conceivably take.

The first of these studies, designated as Assembly 27, Fig. 1, consists of an annular core of "normal" composition and an interior cylindrical core of a reduced height, in which the normal core constituents have been condensed by removing the aluminum which is used to simulate the sodium. This configuration could be hypothesized as resulting from an accident in which the central portion of the core melts, the coolant vaporizes, the central portion collapses to form a condensed or "dense" core at the bottom of the reactor.

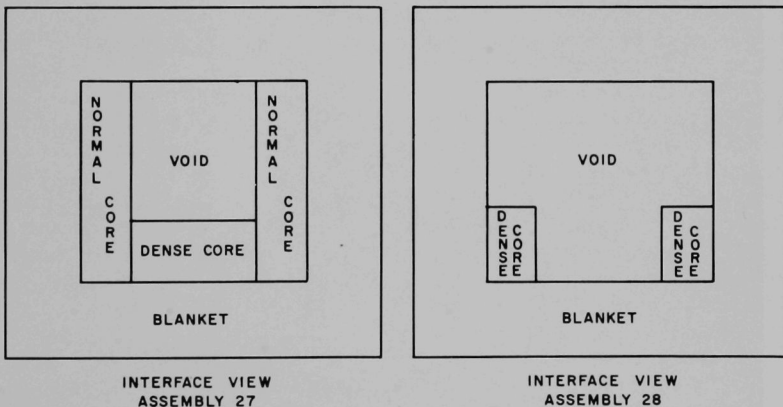


Fig. 1. Interface Views of Assemblies 27 and 28

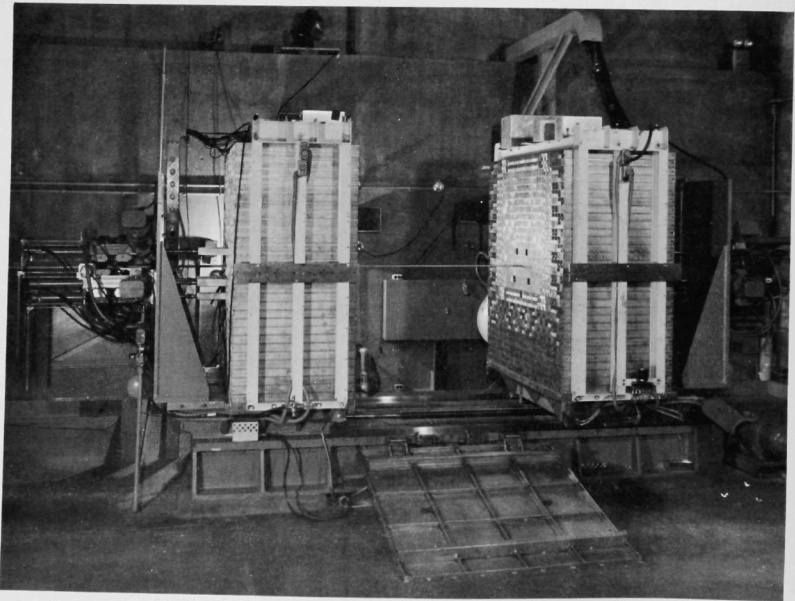
The second study, Assembly 28, Fig. 1, was an annular dense core of reduced height, with a central void. A configuration of this type could result from general core melting and the core collapsing with the central material being ejected from the core region by the vaporizing coolant.

The dimensions of the experiment and the composition of the normal core and blanket utilized in these experiments were similar to those of the previous Enrico Fermi Fast Reactor critical performed in ZPR-III.⁽¹⁾

These results were transmitted to PRDC in preliminary form at the time the experiments were performed in order that the safety analysis by Nicholson⁽⁴⁾ might include these data. Since that time the numerical data have been rechecked and a number of corrections made. In general, these corrections have not altered the shape of the traverse curves greatly, although magnitudes have been shifted in some cases. Since the gradients of the flux and reactivity are the quantities entering the excursion analysis rather than the magnitudes, it is not expected that the new values will alter any conclusions from Nicholson's already completed analysis.

II. DESCRIPTION OF ZPR-III

The ZPR-III is a split-half critical assembly, each half being composed of a 31 square matrix constructed of stainless steel channels, 2.1755 in. (5.526 cm) high, 2.1835 in. (5.546 cm) wide, and 33.5 in. (85.1 cm) long. Into this matrix stainless steel drawers containing the materials composing the experiment are loaded. A complete description of the facility is contained in the Hazard Evaluation Report.⁽⁵⁾ Figure 2 is a view of the facility.



ID-103-2099

Fig. 2. General View of ZPR-III in Shutdown Condition

III. ASSEMBLY 27

To utilize the preferential expansion of the fuel along the axis of the drawers in the ZPR-III as a safety factor in this assembly, the axis of the cylindrical core was oriented vertically at the center (interface) of the machine. This is in contrast to the usual practice of orienting the axis horizontally. To insure cumulative expansion in the positive radial direction of the core, aluminum spacers were placed in the regions designated as void. Figures 3 and 4 are typical drawer-loading diagrams.

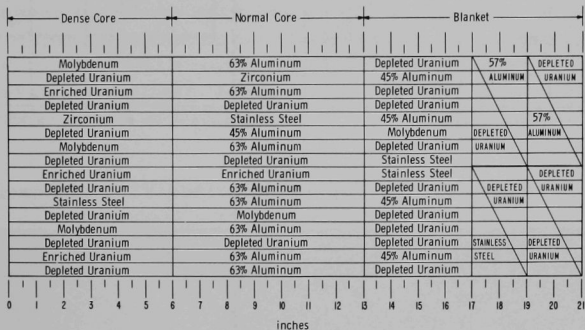


Fig. 3. Assembly 27, Typical Drawer with Dense and Normal Core, and Blanket

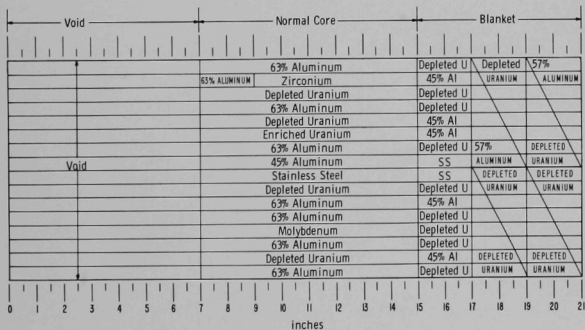


Fig. 4. Assembly 27, Typical Drawer with Void, Normal Core, and Blanket

Figure 5, a top view of one quarter of the reactor, shows the approximate outline of the regions of the experiment and a side view with the critical dimensions. A representative cross section of the core is shown in Fig. 6, where a row of drawers has been partially extracted from the matrix to show the fine detail.

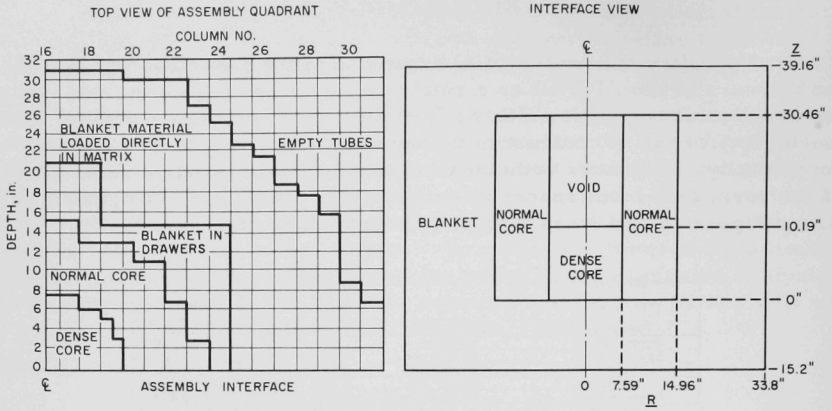
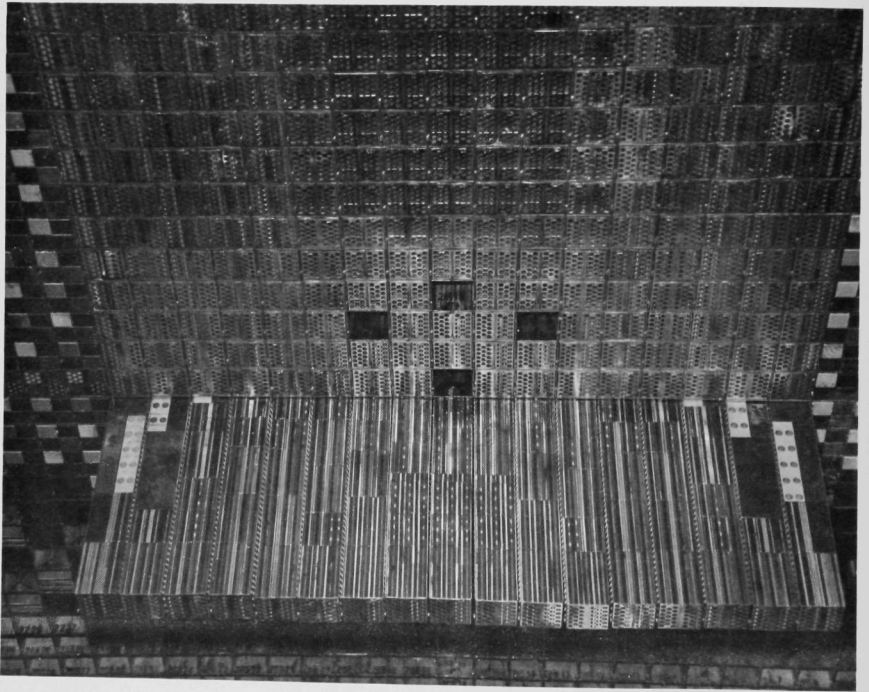


Fig. 5. Assembly 27, Top and Interface View of Assembly



ID-103-2102

Fig. 6. Assembly 27, Representative View through Cross Section of Core

A. Approach to Critical

The approach to critical was made by first loading the dense and normal core regions with depleted uranium occupying the positions of the enriched uranium. In three increments enriched uranium was substituted for depleted uranium in the normal core region. Next, the enriched uranium was substituted in small increments in the dense core region, progressing from the bottom to the top row. To arrive at a critical loading, and at the same time permit the construction of a top row of uniform level height in the dense core region within the limits of inventory, it was necessary to expand the dense core radially in the three central drawers of both halves. This was done in the final loadings by extending the dense region and displacing the normal region radially by 0.5 in. The mass additions and the associated inverse count rates for two counting channels, c_1 and c_2 , are tabulated in Table I.

Table I

APPROACH TO CRITICAL, ASSEMBLY 27

Loading No.	Mass Loaded (kg)	Control Rods "Out"		Control Rods "In"	
		$(1/c_1) \times 10^5$	$(1/c_2) \times 10^5$	$(1/c_1) \times 10^5$	$(1/c_2) \times 10^5$
3	299.99	882	306	882	320
4	316.59	655	301	752	294
5	333.19	450	248	439	247
6	341.78	353	210	321	209
7	349.78	236	161	250	169
8	358.38	155	112	159	112
9	366.38	88	64	81	60
10	371.36	64	48	49	37
11	375.62	32.5	24.2	13.3	9.5
12	377.24	22.5	16.0	7.9	5.6
13	379.34	13.3	9.8	Critical	
14	380.574			+59.4 lh supercritical ^a	
15	381.434			+171.6 lh supercritical ^b	

^aDetermined by calibration of control rod.

^bEntire dense core region loaded to 4.75 drawers high.

The critical height was calculated from the increment in the U^{235} between loadings 14 and 15, 0.86013 kg, which represented an increase in reactivity of 112.2 lh. Based on an average dense core mass per row of 17.147 kg of U^{235} , this addition represented 4.4708×10^{-4} row/lh. As the total excess reactivity of loading 15 was 171.6 lh, the critical height was 4.673 rows at 2.1755 in./row, or a critical height of 10.17 in. The critical mass was then 80.13 kg in the dense core and 299.99 kg of U^{235} in the normal core. The composition and average dimensions of the various zones are

At each point in the traverses the number of traverse fission counter counts per 10^4 counts on a stationary reference fission counter were recorded. The axial fission rate at an elevation Z of 5.44 in., measured from the bottom of the core, was used to normalize the axial fission rate to unity. The radial traverses were then normalized to the axial traverse at their points of intersection. The rates at the points of intersection were determined graphically. This was necessary because a post-experimental X ray of the traverse counters redefined the center of the sensitive length and a more precise measurement of the matrix center spacing was utilized in the computation of the data. The discrepancy due to the axial traverse tube being at a radial position of ≈ 0.3 in. was neglected due to the small gradient of the radial traverses at the center of the core.

The traverse data are tabulated in Tables III and IV, and graphed in Figs. 8 through 15.

Table III

ASSEMBLY 27, AXIAL TRAVERSE,
 U^{235} FISSION COUNTER, AT
 R = 0.3 in.

Axial Position ^a	Relative Count Rate ^b	Axial Position ^a	Relative Count Rate ^b
-0.96	0.551	9.92	0.664
0.13	0.652	10.51 ^c	0.586
1.20	0.775	11.10 ^c	0.568
2.31	0.889	12.10	0.534
3.37	0.959	12.11 ^c	0.523
4.48	0.998	14.27	0.476
5.57	1.000	20.80	0.366
6.65	0.965	27.34	0.276
7.71 ^c	0.918	30.09 ^c	0.255
7.74	0.908	31.69	0.228
8.31 ^c	0.849	32.51 ^c	0.199
8.83	0.785	34.31 ^c	0.158
9.31 ^c	0.739	38.22	0.094

^a Measured from bottom of core.

^b Arbitrarily normalized to unity at Z = 5.57 in.

^c Indicated points were taken in random order to determine reproducibility.

Table IV

ASSEMBLY 27, RADIAL TRAVERSES, U²³⁵ FISSION COUNTER

Traverses Normalized to Axial Fission Counter Traverse

Radial Position ^a	Relative Count Rate							
	1.09	3.26	5.44	Axial Position		14.14	20.67	20.62 ^c
				7.61	9.79			
21.15	0.074	0.091	0.094	0.098	0.100	0.090	0.073	0.073
18.15		0.148	0.163	0.167				
17.15		0.174	0.189	0.198	0.204	0.183	0.145	0.141
16.15		0.208	0.224	0.238	0.245	0.216	0.169	0.172
15.45	0.200				0.266	0.244	0.184	0.186
15.15		0.253	0.263	0.280				
14.65		0.264		0.296	0.311	0.264	0.210	0.211
14.15		0.278	0.305	0.310				
13.15	0.275	0.322	0.350	0.354				
12.90					0.371	0.326	0.254	0.255
12.15			0.384					
11.65	0.327							
11.15		0.404	0.436	0.438				
10.35					0.464	0.400	0.312	0.313
10.15			0.469					
9.15		0.499	0.522	0.515				
8.15		0.556	0.582	0.584				
7.75	0.490	0.576		0.591	0.544	0.456	0.354	0.362
7.15		0.613	0.639	0.619	0.557	0.469	0.365	0.360
6.65		0.651		0.678				
6.15	0.569	0.689	0.724	0.687	0.595	0.471	0.369	0.368
5.15			0.815			0.479	0.364	0.376
4.15		0.830	0.850	0.798				
3.95	0.693				0.641	0.480	0.366	0.363
3.15			0.930					
2.15		0.924	0.953	0.887		0.484	0.366	0.367
1.15		0.919	0.980	0.886				
0.15	0.792	0.956	1.01	0.915	0.683	0.478	0.369	0.369
-0.85		0.957	0.989					
-1.85		0.951	0.973	0.890		0.483	0.373	0.359
-2.85			0.970					
-3.85	0.767	0.881	0.931	0.835		0.474	0.365	0.373
-4.85		0.809	0.872					
-5.85		0.763	0.811	0.758				
-6.85		0.676	0.732					
-7.45		0.640			0.574	0.468		0.359
-7.85		0.595	0.636	0.628				
-8.85		0.542	0.582					
-9.85			0.518					
-10.85			0.472					
-11.85			0.432	0.439				
-12.85			0.376					
-13.85		0.316	0.342					
-15.15			0.289 ^b		0.295	0.273		0.217
-15.85			0.268					
-16.85			0.219					
-17.55			0.199	0.209				

^aDistance from axis of core ±0.125 inches.^bPosition - 14.85 inches.^cDuplication of traverse to check reproducibility.

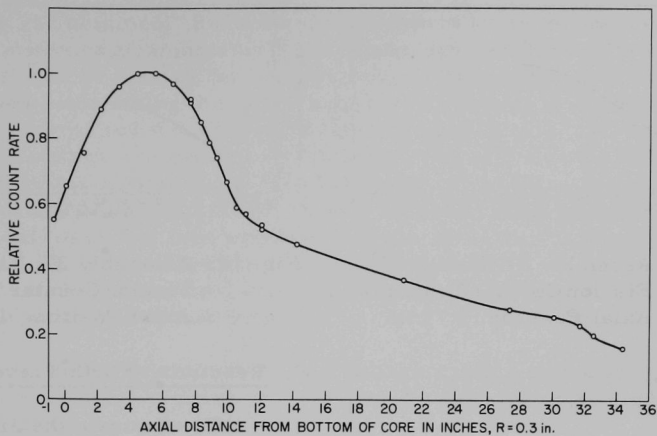


Fig. 8. Assembly 27, Axial U^{235} Fission Counter Traverse

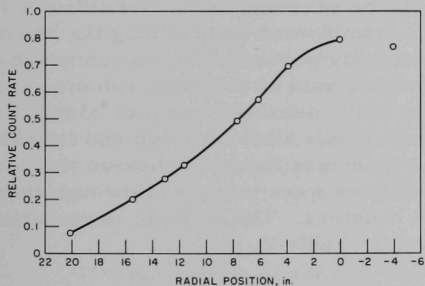


Fig. 9. Assembly 27, Radial U^{235} Fission Counter Traverse; Axial Position, 1.09 in.

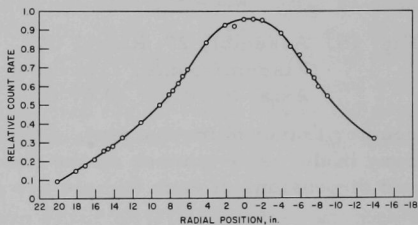


Fig. 10. Assembly 27, Radial U^{235} Fission Counter Traverse; Axial Position, 3.26 in.

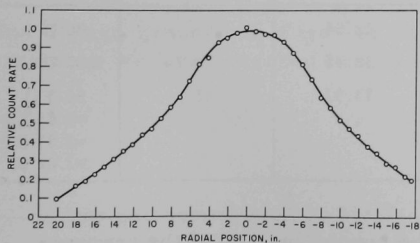


Fig. 11. Assembly 27, Radial U^{235} Fission Counter Traverse; Axial Position, 5.44 in.

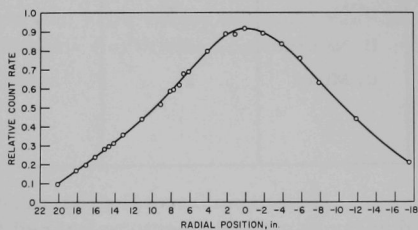


Fig. 12. Assembly 27, Radial U^{235} Fission Counter Traverse; Axial Position, 7.61 in.

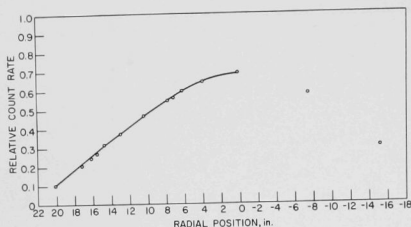


Fig. 13. Assembly 27, Radial U^{235} Fission Counter Traverse; Axial Position, 9.79 in.

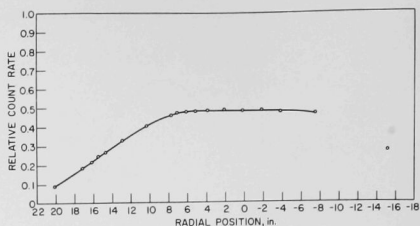


Fig. 14. Assembly 27, Radial U^{235} Fission Counter Traverse; Axial Position, 14.14 in.

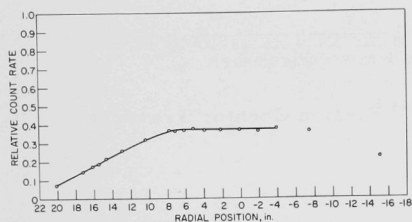


Fig. 15. Assembly 27, Radial U^{235} Fission Counter Traverse; Axial Position, 20.67 in.

counter traverse mechanism. These samples were traversed through the core in the same manner as the fission counters. The isotopic composition and dimensions of each sample are given in Table V.

C. Reactivity Worth Traverses

To eliminate the error due to the degree of reproducibility of half closure and save the time consumed in actually substituting the samples at the various positions within the assembly and determining the reactivity perturbation, as compared with a void of the same volume, $1/2$ -in.-diameter samples of the materials were obtained and fitted to connectors to attach them to the

Table V

REACTIVITY WORTH TRAVERSE SAMPLES

Sample	Approximate Length, in.	Diameter, in.	Uranium Content, gm	Enrichment, %	Analysis, %
U^{235}	0.5	29/64	22.54	93	100 U
U, Natural	1	3/8	32.15	0.7	100 U
U, Mixed	2	29/64	73.93	25	86.5 U ≈7.65 Mo ≈2.87 Zr ≈3.00 SS

The experimental procedure consisted of first traversing with a dummy sample connector attached to the connecting rod of the traverse mechanism and determining the perturbation. Each of the samples was then run and the total perturbation of the sample, connector, and the

connecting rod obtained. Because of the relatively low worth of the perturbation, period measurements were not made; instead, the worth at each point was determined by making the reactor critical at each point at a power level of 0.5 W and determining the perturbation as a function of control rod position. The control rod was then calibrated accurately over the region of interest by period measurements.* The worth per inch was applied to the critical positions obtained to determine the total excess reactivity available in the reactor with the sample or "blank" located at that position. For the radial traverses it was then assumed that the samples and blank were worth zero at $R = 21.0$ in. and for the axial traverses at $Z = 38$ in. The worth of the blank was then subtracted from the sample and the worth normalized to zero at the above-mentioned points.

In the radial position $R = 21.0$ in., the samples were 5.5 in. from the core, and in the axial position, $Z = 38$ in., the samples were 7.44 in. into the top axial blanket.

The relative accuracy of the data is between 0.05 and 0.15 lh. This estimate of the error is based upon the reproducibility of the critical position of the control rod and the sample. While taking the data using the U-mixed sample, points were rerun by repeating traverse positions out of sequence. The five positions which were repeated, at $R = 0$, gave an average error of control rod position of 0.0016 in., with the largest error being 0.005 in. This is relatively independent of sample-position error due to the small worth gradient. A reproducibility of critical position of control rod position of approximately 0.005 in. is assumed for ZPR-III. When the maximum rod worth per inch is applied to this position error of 0.005 in., the uncertainty is ± 0.09 lh.

Measurements of sample-position error of this and other assemblies has been less than ± 0.125 in. This error when applied to regions of large worth gradient of both sample and blank could produce uncertainties of $\approx \pm 0.15$ lh. To reduce the sample-blank position error each point in the traverses was approached from the same direction.

The reactivity worth traverses are tabulated in Tables VI, VII, VIII and IX, and graphed in Figs. 16 through 32. The radial natural uranium traverses were not graphed because of the low worth and scatter.

* ZPR-III Inhour Curve No. 4, based upon APDA Tech. Memo No. 15, $\beta_{\text{eff}} = 0.00687$, 448 lh/%, 308 lh/\$ was used.

Table VI

 ASSEMBLY 27, AXIAL WORTH TRAVERSES
 Sample Worths (Ih) vs. Axial Position^a

Axial Position (in.)	0.5-in. U ²³⁵ Sample	2-in. U-Mixed Sample	1-in. Natural U Sample	
	Worth	Worth	Axial Position (in.)	Worth
-3.29	1.22 ± 0.16		-0.84	0.26 ± 0.14
-1.11	2.04 ± 0.16	2.20 ± 0.16	1.16	0.40 ± 0.14
-0.03	2.89 ± 0.16	3.13 ± 0.16	3.16	-0.02 ± 0.14
1.06	4.10 ± 0.16	3.89 ± 0.16	4.16	-0.18 ± 0.14
2.15	4.95 ± 0.16	4.35 ± 0.16	5.34	-0.15 ± 0.14
3.24	5.63 ± 0.16	4.65 ± 0.16	6.44	-0.02 ± 0.14
4.16		4.76 ± 0.16	7.13	0.07 ± 0.14
4.33	6.12 ± 0.16	4.79 ± 0.14	8.56	0.39 ± 0.15
4.66		4.77 ± 0.14	10.02	0.63 ± 0.15
4.91		4.81 ± 0.14	10.66	0.49 ± 0.15
5.16		4.88 ± 0.14	11.86	0.27 ± 0.15
5.42	6.18 ± 0.17	4.86 ± 0.14	14.16	0.24 ± 0.15
5.66		4.85 ± 0.14	20.56	0.07 ± 0.14
5.91		4.79 ± 0.14	27.14	0.13 ± 0.14
6.16		4.74 ± 0.14	31.40	-0.01 ± 0.14
6.41		4.75 ± 0.16	37.96	0 ^a
6.50	5.85 ± 0.17	4.72 ± 0.16		
6.66		4.71 ± 0.16		
7.12		4.60 ± 0.16		
7.59	4.95 ± 0.17	4.55 ± 0.16		
7.66		4.48 ± 0.16		
8.16		4.36 ± 0.16		
8.68	3.96 ± 0.17	4.21 ± 0.16		
9.77	2.81 ± 0.17	3.53 ± 0.16		
11.95	1.90 ± 0.17	2.14 ± 0.16		
14.08	1.48 ± 0.17	1.63 ± 0.16		
20.66	0.82 ± 0.14	0.78 ± 0.14		
27.19	0.59 ± 0.14	0.36 ± 0.14		
31.54	0.29 ± 0.14	0.20 ± 0.14		
38.07	0 ^a	0 ^a		

^aSample worth assumed zero at indicated positions.

Table VII

 ASSEMBLY 27, RADIAL WORTH TRAVERSES, 0.5-in. U²³⁵ SAMPLE
 Worth (Ih) Relative to 21.0 in.^a

Axial Position Z, in.	Radial Position R, in.									
	21.0	15.3	12.75	10.2	7.6	6.08	3.8	0	-7.6	-15.3
1.09	0 ± 0.14	-0.43 ± 0.14	0.53 ± 0.14	1.00 ± 0.14	1.75 ± 0.16	2.26 ± 0.16	3.20 ± 0.16	3.96 ± 0.14	1.95 ± 0.14	0.63 ± 0.14
3.26	0 ± 0.14	0.38 ± 0.14	0.71 ± 0.14	1.32 ± 0.14	2.17 ± 0.16	3.29 ± 0.16	4.52 ± 0.14	5.42 ± 0.14	2.56 ± 0.15	0.73 ± 0.15
5.44	0 ± 0.14	0.13 ± 0.14	0.49 ± 0.14	1.05 ± 0.14	1.98 ± 0.17	3.13 ± 0.17	4.77 ± 0.14	5.51 ± 0.14	2.23 ± 0.15	0.60 ± 0.15
7.61	0 ± 0.14	0.10 ± 0.14	0.30 ± 0.16	0.53 ± 0.16	1.69 ± 0.16	2.79 ± 0.16	4.02 ± 0.16	4.53 ± 0.14	1.97 ± 0.15	0.07 ± 0.15
9.79	0 ± 0.15	0.26 ± 0.15	0.67 ± 0.15	1.11 ± 0.15	1.60 ± 0.15	1.88 ± 0.15	2.25 ± 0.15	2.96 ± 0.15	1.71 ± 0.14	0.47 ± 0.14
14.14	0 ± 0.14	0.32 ± 0.14	0.55 ± 0.14	0.77 ± 0.14	0.96 ± 0.14	0.88 ± 0.14	1.02 ± 0.14	1.10 ± 0.14	0.99 ± 0.14	-0.49 ± 0.14
20.67	0 ± 0.14	0.37 ± 0.14	0.51 ± 0.14	0.65 ± 0.14	0.72 ± 0.14	0.81 ± 0.14	0.77 ± 0.14	0.79 ± 0.14	0.69 ± 0.14	0.36 ± 0.14

^aWorth at 21.0 in. assumed to be zero.

Table VIII

 ASSEMBLY 27, RADIAL WORTH TRAVERSE, 2-in. NATURAL URANIUM SAMPLE
 Worth (Ih) Relative to 21.0 in.^a

Axial Position Z, in.	Radial Position, in.									
	21.0	15.3	12.75	10.2	7.6	6.08	3.8	0	-7.6	-15.3
5.44	0 ± 0.14	-0.14 ± 0.14	-0.26 ± 0.14	-0.14 ± 0.14	-0.09 ± 0.14	-0.11 ± 0.14	-0.19 ± 0.14	-0.51 ± 0.14	-0.23 ± 0.14	-0.08 ± 0.14
9.79	0 ± 0.14	0.10 ± 0.14	0.05 ± 0.14	0 ± 0.14	0.02 ± 0.14	-0.07 ± 0.14	0.24 ± 0.15	0.68 ± 0.15	0 ± 0.14	0.03 ± 0.14

^aWorth at 21.0 in. assumed to be zero.

Table IX
 ASSEMBLY 27, RADIAL WORTH TRAVERSES, 2-in. U-MIXED SAMPLE
 Worth (1h) Relative to 21.0 in.^a

Axial Position Z, in.	Radial Position R, in.									
	21.0	15.3	12.75	10.2	7.6	6.08	3.8	0	-7.6	-15.3
1.09	0 ± 0.14	0.26 ± 0.14	0.60 ± 0.14	0.91 ± 0.14	1.70 ± 0.15	2.39 ± 0.15	3.09 ± 0.15	4.01 ± 0.14	2.22 ± 0.14	
3.26	0 ± 0.14	0.33 ± 0.14	0.68 ± 0.14	1.26 ± 0.15	2.20 ± 0.15	2.85 ± 0.15	3.94 ± 0.15	4.62 ± 0.14	2.27 ± 0.14	0.60 ± 0.14
5.44	0 ± 0.14	0.14 ± 0.14	0.56 ± 0.14	0.93 ± 0.14	2.04 ± 0.16	3.00 ± 0.16	3.86 ± 0.16	4.70 ± 0.15	2.26 ± 0.15	0.41 ± 0.15
7.61	0 ± 0.14	0.26 ± 0.14	0.44 ± 0.14	0.97 ± 0.15	1.91 ± 0.15	2.48 ± 0.15	3.45 ± 0.15	4.00 ± 0.14	1.77 ± 0.14	0 ± 0.14
9.79	0 ± 0.14	0.24 ± 0.14	0.54 ± 0.14	0.98 ± 0.14	1.23 ± 0.15	1.65 ± 0.15	2.42 ± 0.15	3.39 ± 0.15	1.55 ± 0.14	0.32 ± 0.14
14.14	0 ± 0.14	0.25 ± 0.14	0.44 ± 0.14	0.59 ± 0.14	0.69 ± 0.14	0.82 ± 0.14	1.11 ± 0.14	1.42 ± 0.14	0.78 ± 0.14	0.23 ± 0.14
20.67	0 ± 0.14	0.36 ± 0.14	0.50 ± 0.14	0.73 ± 0.14	0.79 ± 0.14	0.92 ± 0.14	1.10 ± 0.14	1.12 ± 0.14	0.68 ± 0.14	0.51 ± 0.14

^a Worth at 21.0 in. assumed to be zero.

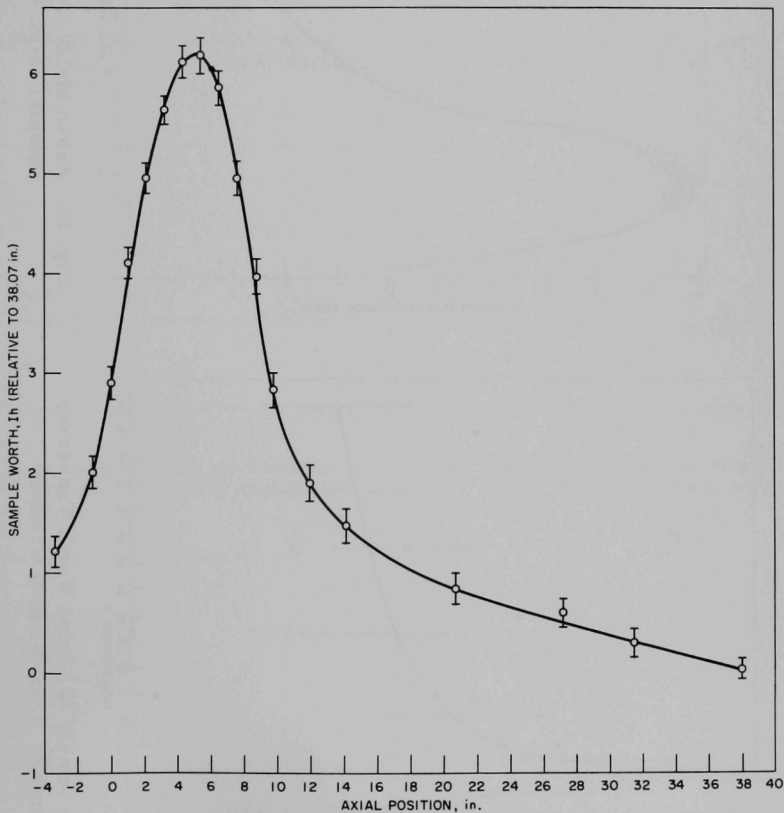


Fig. 16. Assembly 27, Axial Worth Traverse;
 Sample: 0.5-in. U²³⁵

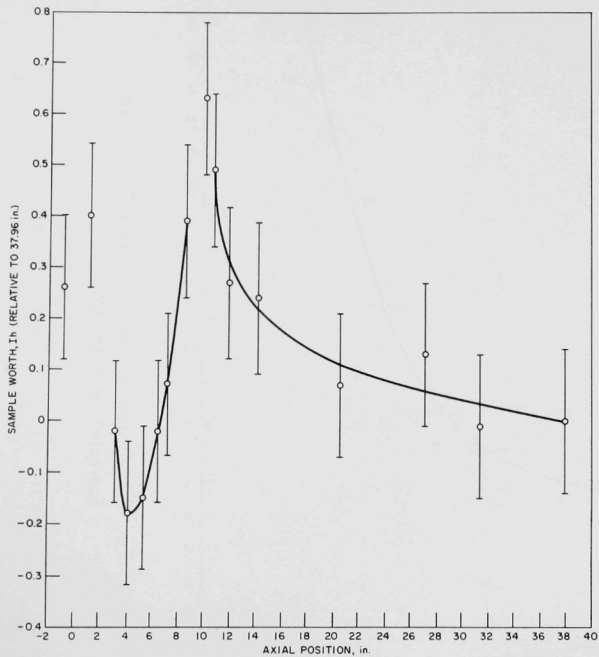


Fig. 17. Assembly 27, Axial Worth Traverse;
Sample: 1-in. Natural Uranium

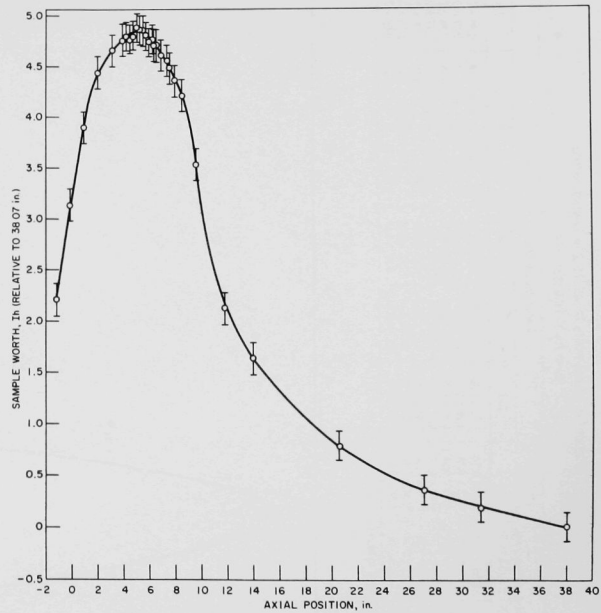


Fig. 18. Assembly 27, Axial Worth Traverse;
Sample: 2-in. U-mixed

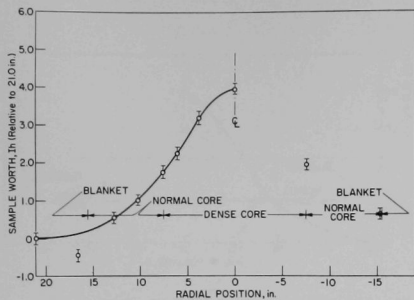


Fig. 19. Assembly 27, Radial Worth Traverse;
Sample: 0.5-in. U^{235} ; Axial Position,
1.09 in.

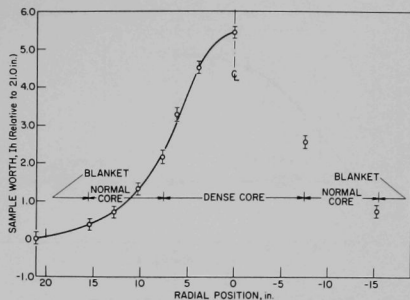


Fig. 20. Assembly 27, Radial Worth Traverse;
Sample: 0.5-in. U^{235} ; Axial Position,
3.26 in.

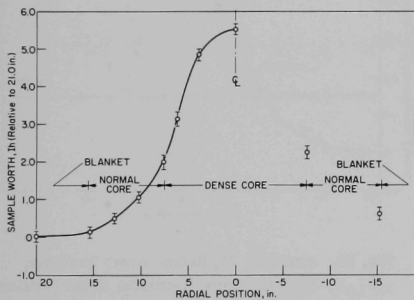


Fig. 21. Assembly 27, Radial Worth Traverse;
Sample: 0.5-in. U^{235} ; Axial Position,
5.44 in.

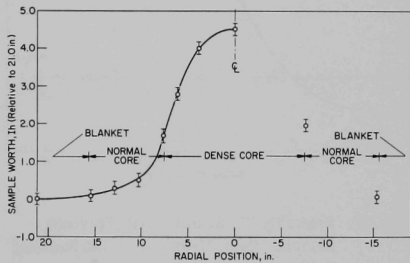


Fig. 22. Assembly 27, Radial Worth Traverse;
Sample: 0.5-in. U^{235} ; Axial Position,
7.16 in.

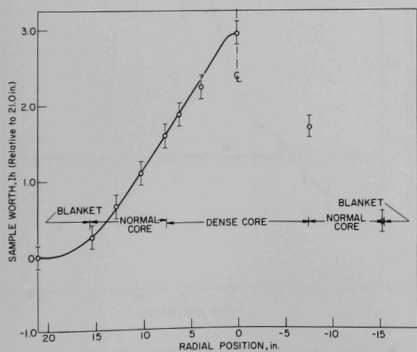


Fig. 23. Assembly 27, Radial Worth Traverse;
Sample: 0.5-in. U^{235} ; Axial Position,
9.79 in.

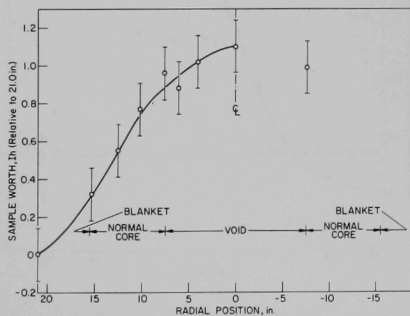


Fig. 24. Assembly 27, Radial Worth Traverse;
Sample: 0.5-in. U^{235} ; Axial Position,
14.14 in.

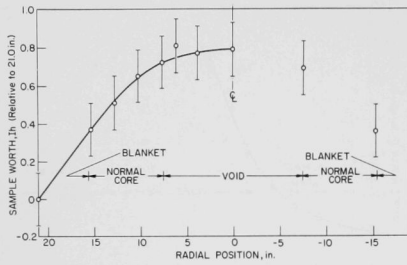


Fig. 25. Assembly 27, Radial Worth Traverse;
Sample: 0.5-in. U^{235} ; Axial Position,
20.67 in.

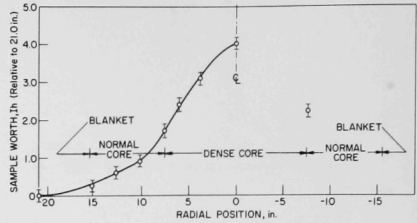


Fig. 26. Assembly 27, Radial Worth Traverse;
Sample: 2-in. U-mixed; Axial Position,
1.09 in.

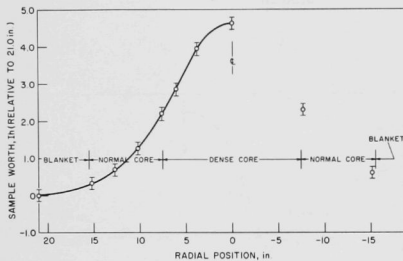


Fig. 27. Assembly 27, Radial Worth Traverse;
Sample: 2-in. U-mixed; Axial Position,
3.26 in.

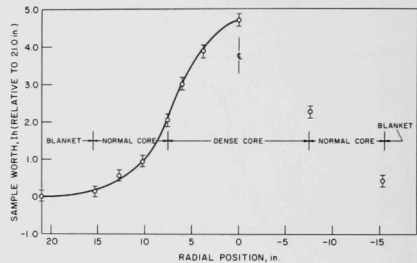


Fig. 28. Assembly 27, Radial Worth Traverse;
Sample: 2-in. U-mixed; Axial Position,
5.44 in.

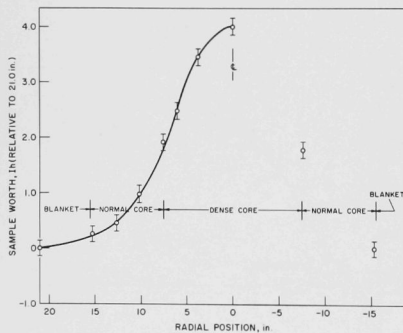


Fig. 29. Assembly 27, Radial Worth Traverse;
Sample: 2-in. U-mixed; Axial Position,
7.61 in.

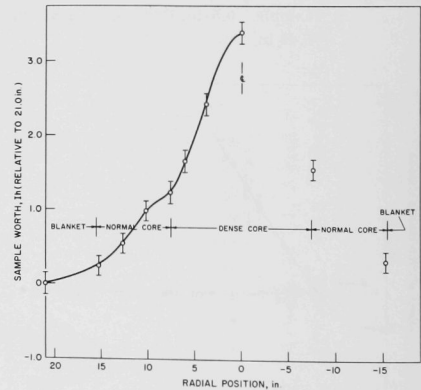


Fig. 30. Assembly 27, Radial Worth Traverse;
Sample: 2-in. U-mixed; Axial Position,
9.79 in.

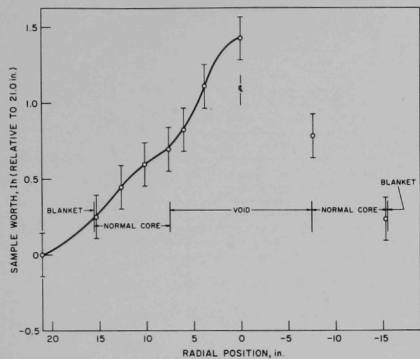
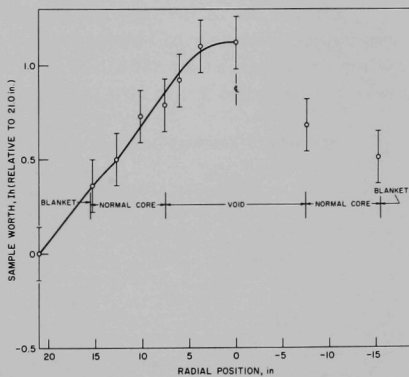


Fig. 31

Assembly 27, Radial Worth Traverse; Sample: 2-in. U-mixed; Axial Position, 14.14 in.

Fig. 32

Assembly 27, Radial Worth Traverse; Sample: 2-in. U-mixed, Axial Position, 20.67 in.



IV. ASSEMBLY 28

Assembly 28 was oriented with the axis of its cylinder vertical in the same manner as Assembly 27. Figure 33 is a typical drawer loading diagram.

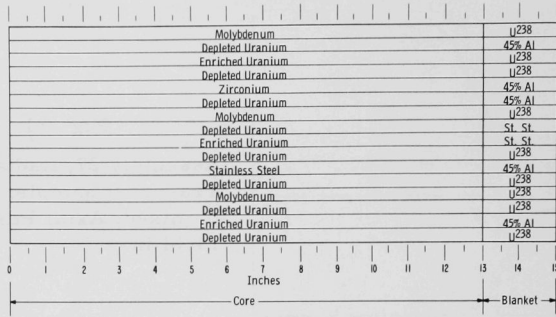


Fig. 33. Assembly 28, Typical Core Drawer

Figure 34 is a top view of one-quarter of the reactor, showing the approximate outlines of the regions of the experiment, and a side view, showing the critical dimensions. In Fig. 35 a row of drawers has been partially extracted from the matrix to show the fine detail.

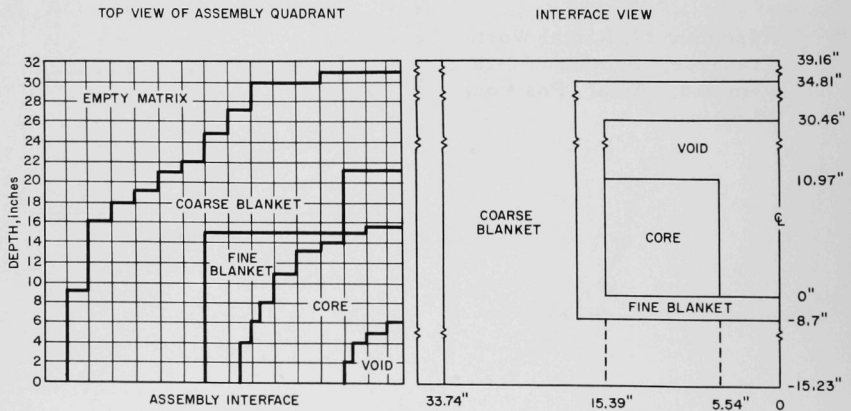
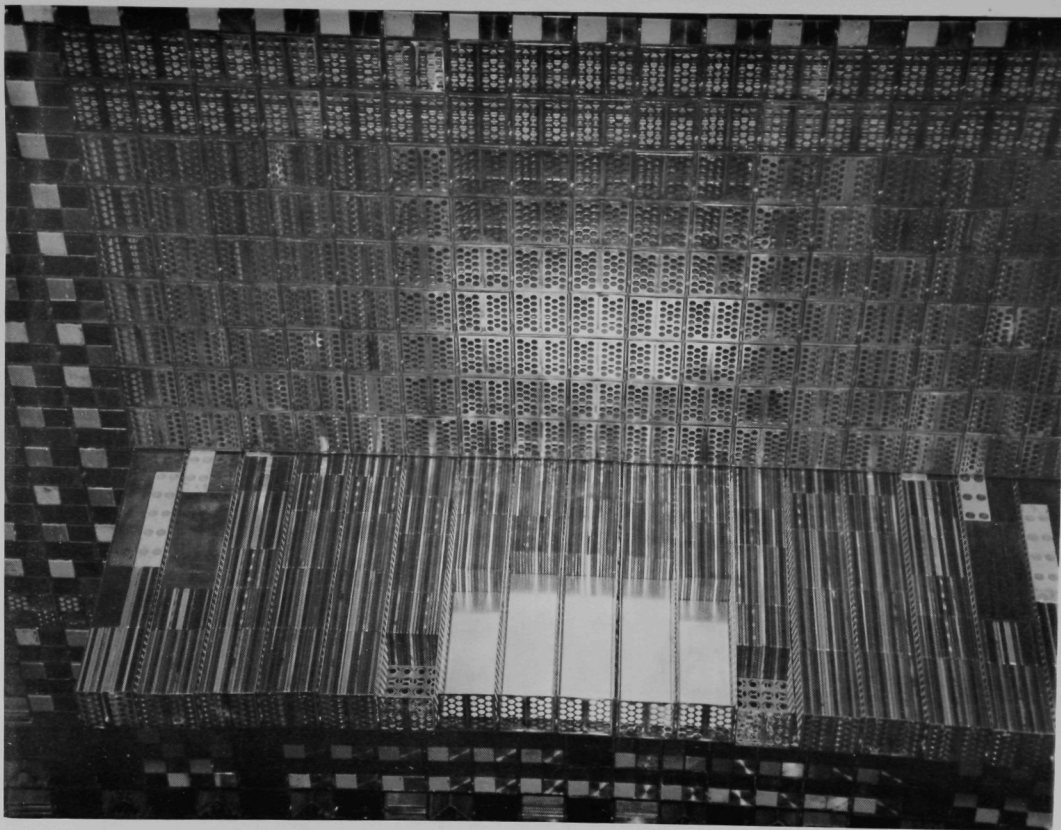


Fig. 34. Assembly 28, Top and Interface View of Assembly



ID-103-2101

Fig. 35. Assembly 28, Representative View through Core Cross Section

A. Approach to Critical

The approach to critical was made by loading the zone to be occupied by the dense core with aluminum spacers and, in steps, constructing the dense core from the bottom, fine axial blanket upward until criticality was achieved. A full-drawer layer of the dense core contained 61.0608 kg of U^{235} . Table X gives the count rate obtained from the proportional counters and the U^{235} mass at each stage of the approach to critical.

Table X
APPROACH TO CRITICAL - ASSEMBLY 28

Loading Number	Mass U^{235} kg	Rods Out				Rods In			
		C_1 (cpm)	C_2 (cpm)	$(1/C_1) \times 10^5$	$(1/C_2) \times 10^5$	C_1	C_2	$(1/C_1) \times 10^5$	$(1/C_2) \times 10^5$
1	61.06	223	99	449	1010	220	89	455	1124
2	122.12	244	118	410	848	244	115	410	870
3	166.73	329	142	304	704	347	137	288	730
4	205.62	452	164	221	610	469	173	213	578
5	244.24	819	265	122	377	870	271	115	369
6	272.41	1457	405	68.6	247	1683	445	59.4	225
7	297.93	4760	1169	21	85.6	7786	1843	12.8	54.2
8	305.3	8433	1985	11.9	50.4	23090	5219	4.33	18.9
9	308.98	10515	2499	9.5	40.0	56542	12644	1.77	7.91
10	313.52	← Critical →							

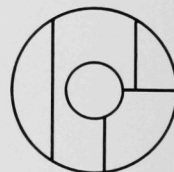
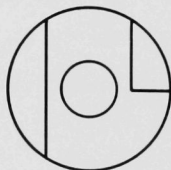
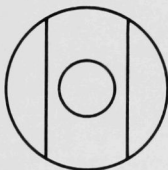
The system achieved criticality with an incomplete layer of fuel. Two experiments (see arrangement in Fig. 36) were performed in which

LOADING NO. 28-10
REACTIVITY 107.8 Ih

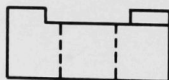
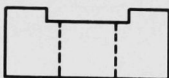
28-11
51.5 Ih

28-12
221.7 Ih

TOP VIEW



SIDE VIEW



28-10/28-11, Lost 56.3 Ih. Therefore flattening the whole core would lose 225.2 Ih and leave the core 117.4 Ih subcritical at a height of 10.8775 in.

28-11/28-12, Gained 170.2 Ih or 1349.4 Ih/in.
Therefore, 117.4 Ih = 0.087 in.
Critical at height = 10.8775 + 0.087 in. = 10.97 in.
Critical mass = 307.62 kg.

Fig. 36. Assembly 28, Core Configurations Used in Estimating Critical Mass

one-fourth of the fuel then in the top layer was removed, reducing the excess reactivity from 107.8 lh to 51.5 lh, or an estimated -117.4 lh if the entire top row had been removed. Then, 23.17% of a quarter of a layer was added in one quadrant, increasing the reactivity to 221.7 lh for a calculated 1349.38 lh/in. of uniform fuel height. The 117.4 lh subcritical at 5 rows high represents 0.087 in. of core height that would be required to make the reactor critical. The critical height is then $(5 \times 2.1775) + 0.087$ or 10.97 in. and the critical mass 307.62 kg U^{235} for a core of uniform height. The critical composition and average dimensions of the various zones are given in Table XI.

Table XI

COMPOSITION OF ASSEMBLY 28 BY ZONES

	Volume Fractions					
	U^{235}	U^{238}	Al	Zr	Mo	SS
Dense Core	0.1406	0.4088		0.0503	0.1524	0.1416
Void			0.0422			0.0932
Blanket	0.0011	0.4870	0.1347			0.210
	CRITICAL DIMENSIONS AND MASS					
Dense Core	Average Inside Radius			5.54 in., 14.07 cm		
	Average Outside Radius			15.39 in., 39.09 cm		
	Average Height			10.97 in., 27.86 cm		
	Critical Mass			307.62 kg of U^{235}		

B. Fission Rate Traverses

The fission rate distributions were measured in the vertical direction 0.3 in. from the axis of the cylinder and radially at five elevations through the core. The counters used were 1/2-in.-diameter U^{235} fission chambers enriched to 93.2% in U^{235} .

Drawers were modified as shown in Fig. 7 to accommodate the traverse guide tube. The counter was positioned at each point to a reproducibility better than ± 0.125 in., and the number of traverse counter counts, at each point, were normalized to 10^4 counts on a stationary reference fission counter. Tables XII and XIII are a tabulation of the radial and axial traverses. These data are graphed in Figs. 37 through 42. The axial and radial data have not been normalized to a common point as was done in Assembly 27.

Table XII

ASSEMBLY 28, AXIAL TRAVERSE, U²³⁵ FISSION COUNTER

At R = 0.3 in.

Axial Position	Relative Count Rate	Axial Position	Relative Count Rate	Axial Position	Relative Count Rate
37.16	0.144	21.16	0.358	6.16	0.882
35.16	0.156	17.16	0.437	5.16	0.908
33.16	0.212	15.16	0.490	4.16	0.926
32.16	0.239	13.16	0.547	3.16	0.924
31.16	0.271	12.16	0.588	2.16	0.908
30.16	0.277	11.16	0.619	1.16	0.897
29.16	0.284	10.16	0.694	0.16	0.880
27.16	0.293	9.16	0.742	-0.84	0.800
25.16	0.308	8.16	0.800	-1.84	0.750
23.16	0.331	7.16	0.837	-2.84	0.663

Table XIII

ASSEMBLY 28, RADIAL TRAVERSES, U²³⁵ FISSION COUNTER

Radial Position Core Axis at 0.00	Relative Count Rate at Axial Position				
	9.79	7.61	5.44	3.26	1.09
21	208	224	229	210	201
18	339	380	381	365	339
16	439	531	550	505	475
15	500	619	655	611	562
14	563	724	744	731	659
13	625	822	882	856	747
11	717	976	1091	1041	899
9	777	1050	1192	1136	1017
7	759	1025	1157	1100	1009
6	736	966	1061	1076	996
5	743	923	995	1013	966
4	740	890	968	972	966
2	719	835	900	919	917
1	724	841	891	917	942
0	719	843	890	917	933
-2	716	850	907	924	949
-4	719	855	942	970	959
-5	730	892	964	970	978
-7	755	1000	1119	1074	984
-9	773	1041	1192	1163	1003
-13	634	855	934	925	796
-15	525	671	719	705	611
-19	304	341	349	344	316

C. Reactivity Worth Traverses

The samples used in these traverses were the 2-in. U-mixed and the 1/2-in. U^{235} traverse samples (see Table XIV). The traverse locations were the same as those of the fission rate traverses. For the radial traverses the worth of the blank and samples were assumed to be zero at a radial distance of 40.25 in. for the U-mixed core sample and at 41.0 in. for the U^{235} sample, and at axial distances of 38.16 in. and 38.41 in., respectively. These data are tabulated in Tables XV and XVI, and graphed in Figs. 43 through 54. Although the general shape of the curves seems apparent, the experimental data are insufficient to define some of the details. Therefore, no attempt has been made to connect the points with a smooth curve. The errors in the individual points are of the order of ± 0.15 lh maximum, while the absolute value of the worths are subject to an error in some traverses due to a variation of the "zero worth" as great as 0.25 lh.

Table XIV

ASSEMBLY 28, AXIAL WORTH TRAVERSES

Worths (lh) vs Axial Position,^a R = 0.3 in.

Axial Position ^b	0.5-in. U^{235} Sample	2-in. U-Mixed Sample	
40.14		0 \pm 0.14	
38.41	0 \pm 0.14 ^a		
38.16		0 \pm 0.14 ^a	0 \pm 0.14 ^a
37.66		0 \pm 0.14	
36.91		0 \pm 0.14	0.07 \pm 0.14
34.91	0 \pm 0.14	0.10 \pm 0.14	
28.91	0.51 \pm 0.14	0.26 \pm 0.14	
23.91	0.52 \pm 0.14	0.40 \pm 0.14	
18.91	0.66 \pm 0.14	0.74 \pm 0.14	
13.91	0.78 \pm 0.15	1.40 \pm 0.15	1.26 \pm 0.15
10.91	1.15 \pm 0.15		
9.76	1.27 \pm 0.15	2.28 \pm 0.14	2.08 \pm 0.14
7.59	1.40 \pm 0.14	1.38 \pm 0.14	1.34 \pm 0.14
5.41	1.40 \pm 0.14	0.92 \pm 0.14	0.73 \pm 0.14
3.24	1.35 \pm 0.14	0.99 \pm 0.14	0.69 \pm 0.14
1.07	1.47 \pm 0.14	1.66 \pm 0.14	1.26 \pm 0.14
-0.61			1.10 \pm 0.14
-1.09			
-1.11		1.30 \pm 0.14	
-1.75			

^aAssumed to be zero at indicated positions.

^bBottom of core at 0.00 in.

Table XV

ASSEMBLY 28, RADIAL WORTH TRAVERSES, 0.5-in. U²³⁵ SAMPLEWorth (Ih) Relative to 41.0 in.,^a Error is ± 0.14 Ih Unless Otherwise Specified

Radial Position, in.	Axial Position, in. ^b				
	9.79	7.61	5.44	3.26	1.09
41.0	0	0	0	0	0
21.0	-0.05	0.10	0.06	0.13	0.04
16.0	0.18	0.62	0.48	0.55 \pm 0.15	0.53
14.0	0.42	1.09	1.15	1.21 \pm 0.15	0.87
12.0	0.53	1.61	1.94	1.71 \pm 0.15	1.18
10.0	0.93	2.01	2.27	2.24 \pm 0.15	1.67
8.0	1.01	2.15	2.39	2.41	1.78
6.0	0.88	1.60	1.87	2.17	1.57
5.0	0.82	1.47	1.56	1.84	1.57
3.0	0.90	1.32	1.23	1.49	1.49
0	0.91	1.30	0.92	1.39	1.32
-7.0	0.95	1.79	2.06	2.30	1.75
-15.0	0.31	0.90	0.74	0.95	0.65

^aWorth at 41.0 in. assumed to be zero.^bBottom of core at 0.0 in.

Table XVI

ASSEMBLY 28, RADIAL WORTH TRAVERSES, 2-in. U-MIXED SAMPLE

Worth (Ih) Relative to 40.25 in.,^a Error is ± 0.14 Ih Unless Otherwise Specified

Radial Position, in.	Axial Position, in. ^b				
	9.79	7.61	5.44	3.26	1.09
40.25	0	0	0	0	0
21.0	0.23	0.07	0.19	0.16	0.20
16.0	0.42	0.82	0.66	0.74	0.48
14.0	0.82	1.27	1.20	1.13	0.92
12.0	1.19	1.52	1.62	1.54	1.21
10.0	1.53	1.98	1.89 \pm 0.15	1.75	1.44
8.0	1.58	1.91	1.81 \pm 0.15	1.73	1.53
6.0	1.58	1.66	1.57 \pm 0.15	1.48	1.32
5.0	1.82	1.60	1.28 \pm 0.15	1.18	
4.0	1.88	1.45	0.94 \pm 0.15	0.86	1.12
0	1.93	1.19	0.16	0.42	1.08
-7.0	1.39	1.58	1.74	1.65	1.39
-15.0	0.61	1.09	1.04	1.03	0.99

^aWorth at 40.25 in. assumed to be zero.^bBottom of core at 0.0 in.

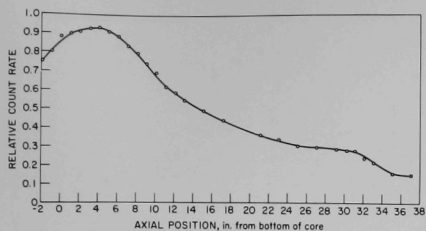


Fig. 37. Assembly 28, Axial U^{235}
Fission Counter Traverse

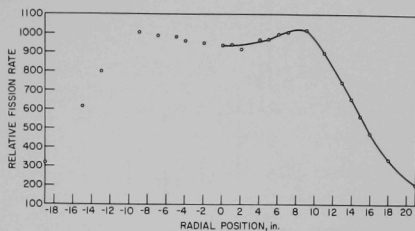


Fig. 38. Assembly 28, Radial U^{235}
Fission Counter Traverse;
Axial Position, 1.09 in.

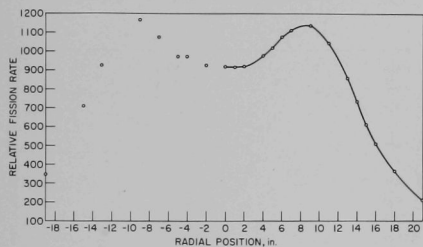


Fig. 39. Assembly 28, Radial U^{235}
Fission Counter Traverse;
Axial Position, 3.26 in.

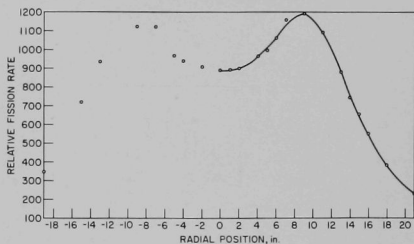


Fig. 40. Assembly 28, Radial U^{235}
Fission Counter Traverse;
Axial Position, 5.44 in.

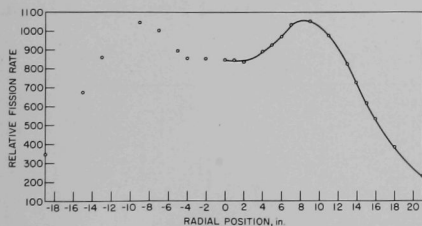


Fig. 41. Assembly 28, Radial U^{235}
Fission Counter Traverse;
Axial Position, 7.61 in.

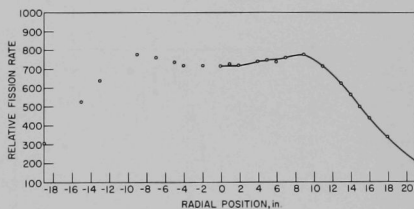


Fig. 42. Assembly 28, Radial U^{235}
Fission Counter Traverse;
Axial Position, 9.79 in.

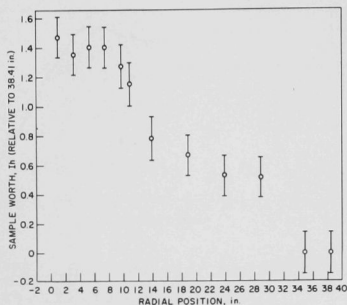


Fig. 43. Assembly 28, Axial Worth Traverse; Sample: 0.5-in. U^{235}

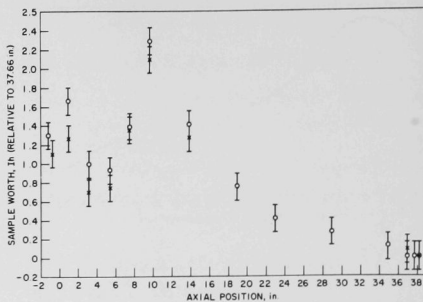


Fig. 44. Assembly 28, Axial Worth Traverse; Sample: 2-in. U-mixed

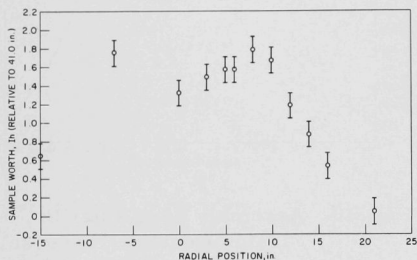


Fig. 45. Assembly 28, Radial Worth Traverse; Sample: 0.5-in. U^{235} , Axial Position, 1.09 in.

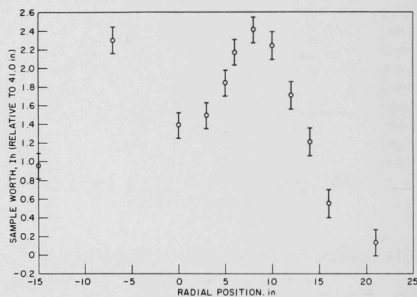


Fig. 46. Assembly 28, Radial Worth Traverse; Sample: 0.5-in. U^{235} , Axial Position, 3.26 in.

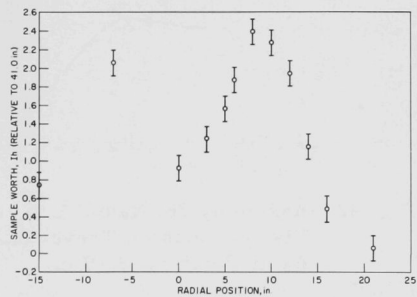


Fig. 47. Assembly 28, Radial Worth Traverse; Sample: 0.5-in. U^{235} , Axial Position, 5.44 in.

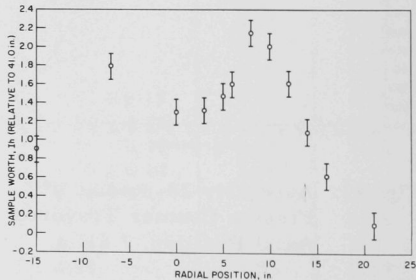


Fig. 48. Assembly 28, Radial Worth Traverse; Sample: 0.5-in. U^{235} , Axial Position, 7.61 in.

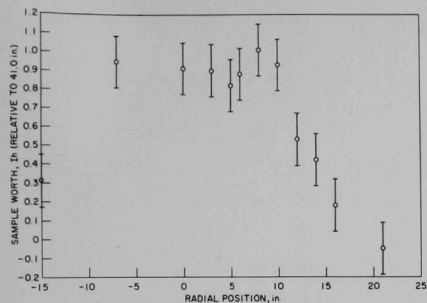


Fig. 49. Assembly 28, Radial Worth Traverse; Sample 0.5-in. U^{235} ; Axial Position, 9.79 in.

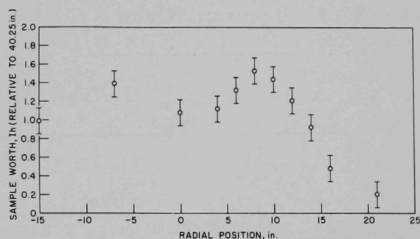


Fig. 50. Assembly 28, Radial Worth Traverse; Sample: 2-in. U-mixed; Axial Position, 1.09 in.

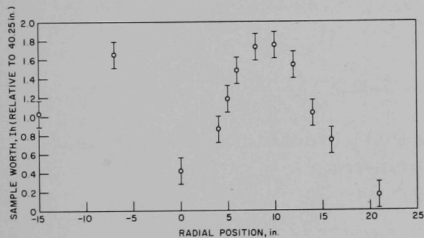


Fig. 51. Assembly 28, Radial Worth Traverse; Sample: 2-in. U-mixed; Axial Position, 3.26 in.

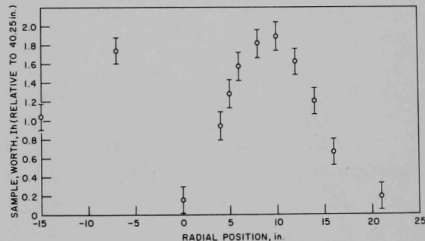


Fig. 52. Assembly 28, Radial Worth Traverse; Sample: 2-in. U-mixed; Axial Position, 5.44 in.

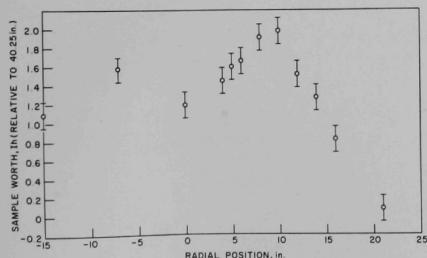


Fig. 53. Assembly 28, Radial Worth Traverse; Sample: 2-in. U-mixed; Axial Position, 7.61 in.

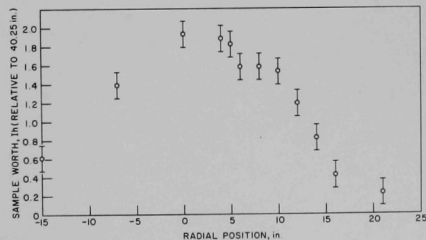


Fig. 54. Assembly 28, Radial Worth Traverse; Sample: 2-in. U-mixed; Axial Position, 9.79 in.

REFERENCES

1. C. E. Branyan, Core A Critical Studies for the Enrico Fermi Atomic Power Plant on ZPR-III, ANL-6629 (Oct 1962).
2. H. A. Bethe and J. H. Tait, An Estimate of the Order of Magnitude of the Explosion When the Core of a Fast Reactor Collapses, UKAEA 56/113.
3. V. Z. Jankus, A Theoretical Study of Destructive Nuclear Bursts in Fast Power Reactors, Physics of Fast and Intermediate Reactors 3, 209, IAEA
4. R. B. Nicholson, Methods for Determining the Energy Release in Hypothetical Reactor Meltdown Accidents, APDA-150 (Dec 1962).
5. R. O. Brittan et al., Hazard Evaluation Report on the Fast Reactor Zero Power Experiment ZPR-III, ANL-6408 (Revised Oct 1961).

ACKNOWLEDGMENT

The authors wish to thank the ZPR-III technicians and student employees who contributed to this experiment.

ARGONNE NATIONAL LAB WEST



3 4444 00009133 0